VTT WORKING PAPERS 182

Riku Pasonen

Energy centre microgrid model

ISBN 978-951-38-7524-4 (URL: http://www.vtt.fi/publications/index.jsp)
ISSN 1459-7683 (URL: http://www.vtt.fi/publications/index.jsp)

JULKAISIJA – UTGIVARE – PUBLISHER

VTT, Vuorimiehentie 5, PL 1000, 02044 VTT
puh. vaihde 020 722 111, faksi 020 722 4374

VTT, Bergsmansvägen 5, PB 1000, 02044 VTT
tel. växel 020 722 111, fax 020 722 4374

VTT Technical Research Centre of Finland, Vuorimiehentie 5, P.O. Box 1000, FI-02044 VTT, Finland
phone internat. +358 20 722 111, fax +358 20 722 4374

Series title, number and
report code of publication

VTT Working Papers 182
VTT-WORK-182

Author(s)
Riku Pasonen

Title
Energy centre microgrid model

Abstract

A simulation model of Energy centre microgrid made with PSCAD simulation software version 4.2.1 has been built in SGEM Smart Grids and Energy Markets (SGEM) work package 6.6. Microgrid is an autonomous electric power system which can operate separate from common distribution system. The idea of energy centre microgrid concept was considered in Master of Science thesis "Community Microgrid – A Building block of Finnish Smart Grid". The name of energy centre microgrid comes from a fact that production and storage units are concentrated into a single location, an energy centre. This centre feeds the loads which can be households or industrial loads. Power direction flow on the demand side remains same compared to the current distribution system and allows to the use of standard fuse protection in the system.

The model consists of photovoltaic solar array, battery unit, variable frequency boost converter, inverter, isolation transformer and demand side (load) model. The model is capable to automatically switch to islanded mode when there is a fault is outside grid and back to parallel operation mode when fault is removed. The modelled system responses well to load changes and total harmonic distortion related to 50Hz base frequency is kept under 1.5% while operating and feeding passive load.

ISBN
978-951-38-7524-4 (URL: http://www.vtt.fi/publications/index.jsp)

Series title and ISSN		Project number
VTT Working Papers 1459-7683 (URL: http://www.vtt.fi/publications/index.jsp)		75700
Date September 2011	Language English	Pages 34 p.
Name of project SGEM, WP6.6 Management and operation of smart grids	Commissioned by VTT, Cleen Oy	
Keywords Smart grid, microgrid, DG, simulation model	Publisher VTT Technical Research Centre of Finland P.O. Box 1000, FI-02044 VTT, Finland Phone internat. +358 20 722 4520 Fax +358 20 722 4374	

Preface

This work was carried out in the Smart Grids and Energy Markets (SGEM) research program Work Package 6.6 coordinated by CLEEN Ltd. with funding from the Finnish Funding Agency for Technology and Innovation. The purpose of this work is to build a simulation model of energy central type of microgrid which was considered in Master of Science thesis “Community Microgrid – A Building block of Finnish Smart Grid”[1] and to use this model to later to investigate possible phenomena caused by large single phase loads and possibilities to control them smartly. This document covers the actual microgrid, not control devices and problematic loads. Single phase loads like heat pumps are to be modelled later in the project. PSCAD® electromagnetic transient software is used as simulation environment for the model.

22.9.2011

Riku Pasonen

Contents

List of symbols

DC	Direct current
gG fuse	General purpose fuse used for over current protection
SOC	State of charge
kWp	Peak power capacity in kilowatts
THD	Total harmonic distortion, used measure overall electric quality
RMS	Root mean square value
LOM	Loss of mains. Situation where grid electricity supply is broken
UI-curve	Chart with current as function of voltage used for characterisation of solar panels
MPPT	Maximum power point tracking

1. Introduction

This chapter describes the operating principle of an energy centre microgrid; an autonomous electric power system. The name of energy centre microgrid comes from a fact that production and storage units are concentrated into a single location, an energy centre. This centre feeds the loads which can be households or industrial loads. Layout of the concept is represented in Figure 1.

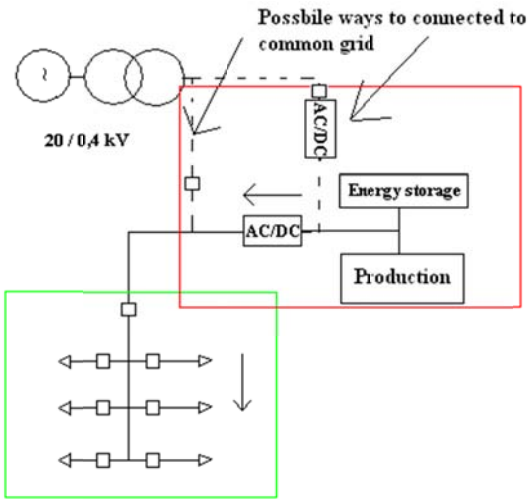

Figure 1. Layout of energy centre microgrid concept.

The obvious advantage which comes with the concept is that regular protection equipment can be used in demand side because direction of the power flow remains the same. Previous figure illustrates two possibilities for the system to be connected to rest of the distribution grid. The option to connect to DC side of the energy centre enables an easy and high response switching between grid supply and the energy centre as this is a series connection in inverter standpoint. Other option is to connect straight to grid and bypass the energy centre when power of the grid is wanted to be used. The later of the options was chosen for the model. Of course there might not be distribution grid available at all.

2. General information about model

This document refers to simulation model “SGEM_VTT_Microgrid.psc” found at SGEM PSCAD model library.

2.1 Requirements and details

Master libraries of vttV42, VYlib42 and master library should be opened before opening the model file. File reference to vttlib.f should be pointed to right location of the file if it is not one folder back from folder structure. Model has been built and tested with PSCAD version 4.2.1 and with free GNU compiler. To be able to open this document from model, linking of PDF-reader software should be done to “Workspace Settings” -> Associations -> Add.

2.2 Limitations of the model

The model is only suitable for one directional power flow simulations through the inverter. Boost converter would have to be switched to buck mode to reverse power flow. Grid side loss of mains (LOM) protection relay is assumed to work as soon as fault is occurs in the grid. Maximum power point tracking system is simplified static voltage control and solar panel model accuracy between irradiation changes could be improved.

2.3 Settings in PSCAD

Following settings have been used in the model.

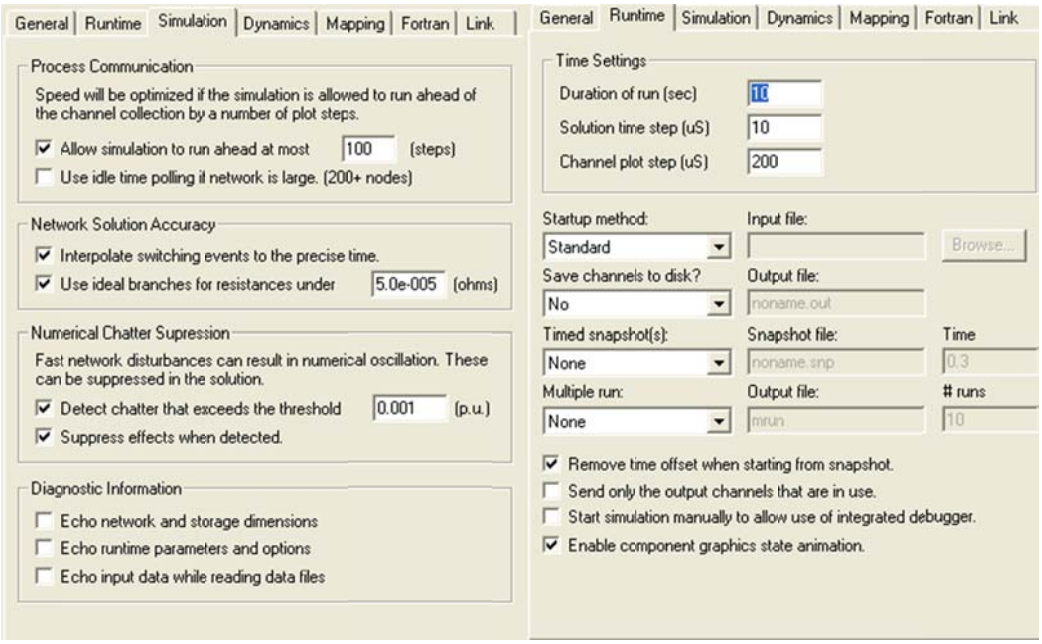

Figure 2. PSCAD settings.

3. Model of Energy centre microgrid

Overall layout of the model in PSCAD simulation software is represented in Figure 3.

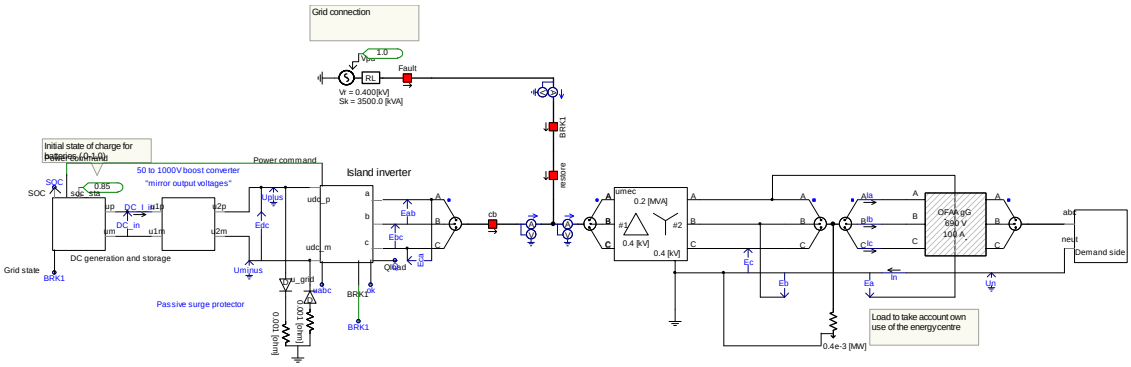

Figure 3. Overall layout of the simulation model.

On far left is the DC side of the system where production and storages are concentrated. Next component from left to right is the DC/DC boost converter which is used to covert 50V DC to 1000V DC. There is passive surge protector modelled by diodes with 0.505 kV forward voltage drops. Next on right from the boost converter there is inverter operating with space vector modulation and isolation transformer with 0.4/0.4 turns ratio. Inverter feeds the load component which is called demand side in the figure. A 3-phase disconnector is located between inverter and loads. Overcurrent protection is done with VTT gG fuse model found at vttV42 library. Grid connection is located between inverter and transformer and modelled using VTT voltage source model found also at vttV42. Documentation for previously built VTT PSCAD models like fuse and space vector modulator can be found at folder SGEM PSCAD MODELS/ Kirjastot/ VTTkirjasto /VTT_help/ of SGEM PSCAD model library.

3.1 Energy centre DC side

Energy centre in this model has a lead-acid battery as storage and solar panel array as production unit. DC-side voltage is around 50V and moving up and down depending on

whether battery is been charged or discharged. Figure 4 displays the layout components in energy centre DC side.

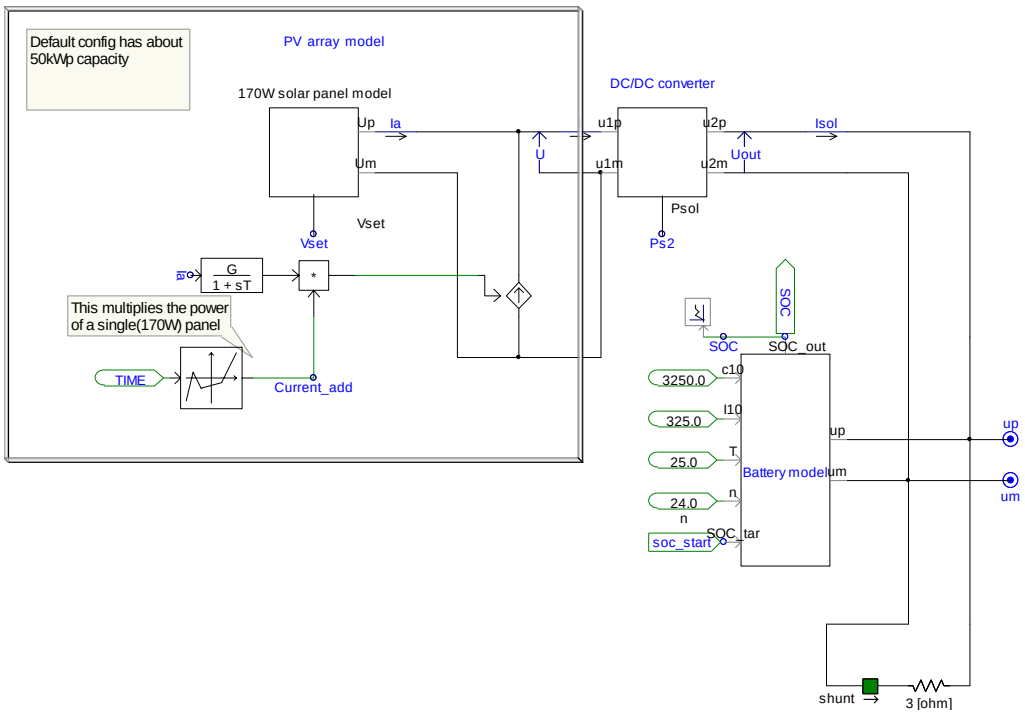

Figure 4. Model of the energy centre DC side.

Solar panel array is outlined with grey line. In addition to solar system and battery model, DC-side includes a boost converter for solar panel connection and overcharge protection shunt load. Also power command is given as output for inverter to know how much power it should output while operating in grid parallel mode.

3.1.1 Overcharge protection and power command logic

Overcharge protection enables shunt load when system is not connected to outside grid and state of battery charge (SOC) is above 0.95. Shunt is removed when SOC decreases to 0.9. Figure 5 displays overcharge protection implementation.

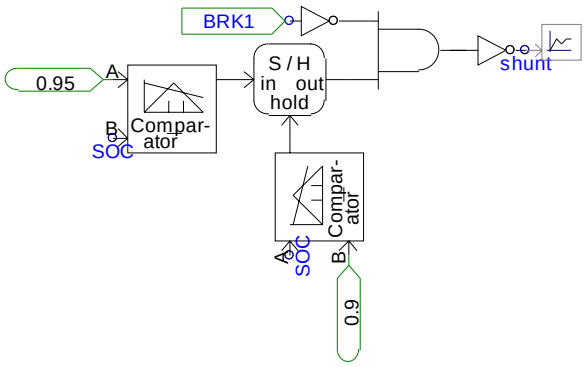

Figure 5. Overcharge protection logic implemented to the model.

Power command for grid parallel operation for inverter is given to be 95% of the power measured from the solar array when SOC is above 0.75. If SOC is lower, power command holds at zero until SOC of battery reaches 0.85. Figure 6 displays power command logic of the model.

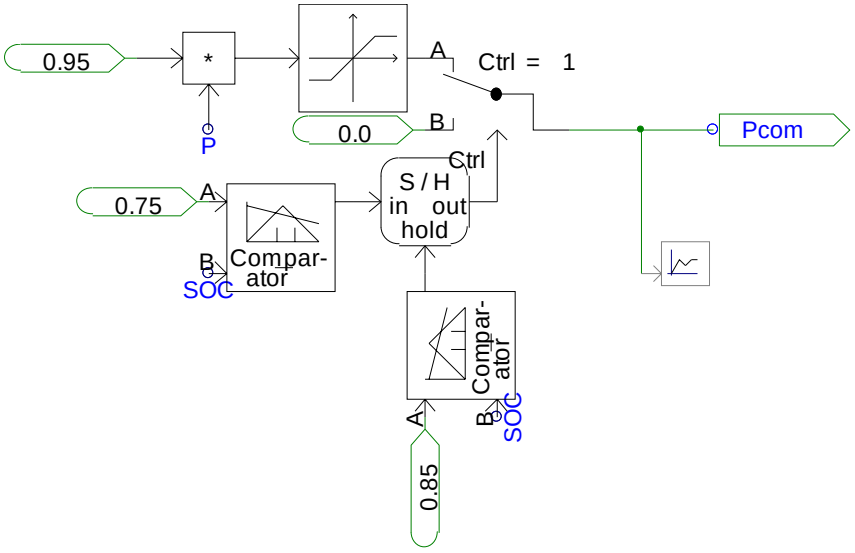

Figure 6. Power command logic.

3.1.2 Battery model

Lead acid battery was chosen as energy storage for this model. Model is based on CIEMAT model which was used in simulations in [2]. The model has different output voltage equations for discharge, charge, and overcharge situation and are calculated according to Figure 7. Reference product for the model is STECO Saphir 3600, of which parameters have been validated also in [2].

$$V_{bat\_d} = n_b \cdot [1{,}965 + 0{,}12 \cdot EDC] - n_b \cdot \frac{|I_{bat}|}{C_{10}} \cdot \left(\frac{4}{1 + |I_{bat}|^{1.3}} + \frac{0{,}27}{EDC^{1.5}} + 0{,}02 \right) \cdot (1 - 0{,}007 \cdot \Delta T)$$

$$V_{bat\_c} = n_b \cdot [2 + 0{,}16 \cdot EDC] + n_b \cdot \frac{I_{bat}}{C_{10}} \cdot \left(\frac{6}{1 + I_{bat}^{0{,}86}} + \frac{0{,}48}{(1 - EDC)^{1{,}2}} + 0{,}036 \right) \cdot (1 - 0{,}025 \cdot \Delta T) \quad (4)$$

$$V_{bat\_oc} = n_b \cdot V_g + n_b \cdot (V_{ec} - V_g) \cdot \left[1 - \exp\left(\frac{t - t_g}{\tau_g} \right) \right]$$

Figure 7. Voltage equations in battery model. d=discharge, c=charge and oc= overcharge [2].

Voltage components of overcharge equation are displayed in Figure 8.

$$\begin{cases} V_{ec} = \left[2{,}45 + 2{,}011 \cdot \ln\left(1 + \frac{I_{bat}}{C_{10}} \right) \right] \cdot (1 - 0{,}002 \cdot \Delta T) \\ V_g = \left[2{,}24 + 1{,}97 \cdot \ln\left(1 + \frac{I_{bat}}{C_{10}} \right) \right] \cdot (1 - 0{,}002 \cdot \Delta T) \\ \tau_g = \frac{1{,}73}{1 + 852 \cdot \left(\frac{I_{bat}}{C_{10}} \right)^{1{,}67}} \end{cases}$$

Figure 8.Voltage components to overcharge equation [2].

Equation 1 represents calculation of SOC by subtracting Q_d, discharged charge. C_{bat} in equation 1 is instantaneous capacity which is calculated by equation 2.

$$EDC = 1 - \frac{Q_d}{C_{bat}}$$

Equation 1. State of charge calculation [2].

$$\frac{C_{bat}}{C_{10}} = \frac{1.67}{1 + 0.67 \cdot (\frac{I_{bat}}{I_{10}})^{0.9}} \cdot (1 + 0.005 \cdot \Delta T)$$

Equation 2. Calculation of instantaneous capacity [2].

Input parameters for the battery model are given with constants to model with outside data connectors (on the left of the model block) in following order going from up to down.

C10 = Charge capacity in Ah when battery is discharged for 10h.
I10 = Current that can be drawn for 10h.
T = Temperature in ºC
N = Number of cells in series
SOC_tar = Initial state of charge for the battery (0 to 1.0)
(given in main page, displayed in Figure 3.)

3.1.3 Solar panel model

Solar array model is based on single 170Wp PV model which is scaled up to 50 kWp to represent an array. Panels in array are connected in parallel. The reasons for choosing parallel connection for panels over series connection are explained in chapter 3.1.4. Panel chosen for simulations is Photowatt 1650 panel. Data for model was collected from [3]. The principle for the solar panel model is to use multiple diodes with resistances in parallel to mimic UI-curve for the panel. This method was introduced in [4]. Performance of panel reflects panel performance in standard operating conditions. Figure 9 represents PSCAD model of the solar panel.

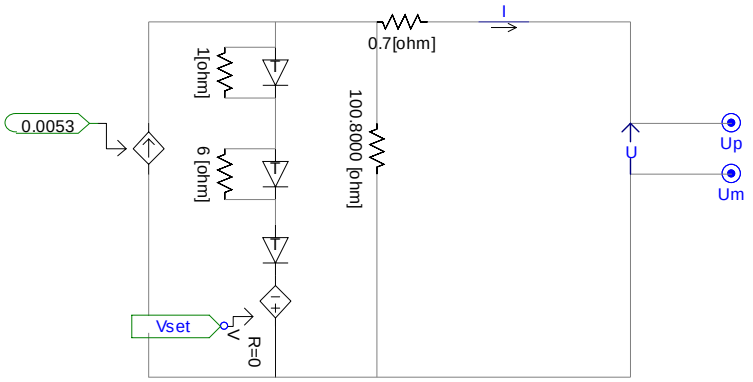

Figure 9. Model of solar panel.

The panel model was tested with current sweep method using variable resistor. Figure 10 represents results of the testing. X-axis represents voltage and Y-axis current. Blue curve is the UI-curve and green is a power curve in 100W scaling.

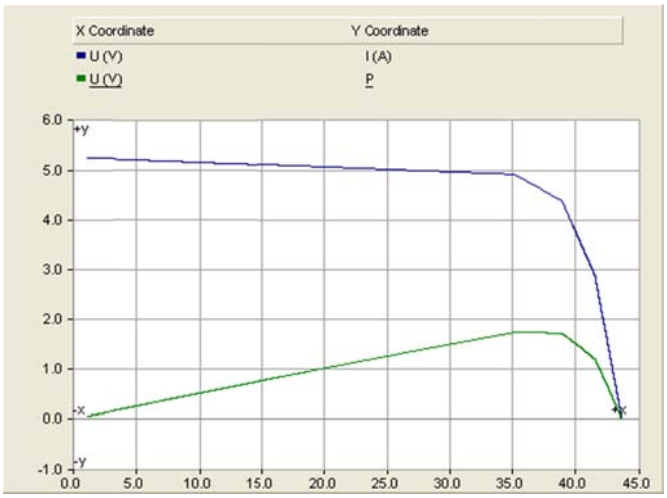

Figure 10. Power 100W (green) and current A (blue) curves of the panel at different voltages.

Conditions with irradiation are modelled by adjusting reverse voltage source (Vset) to mimic lower open circuit voltages. The voltage does not change very much and larger changes occur in amount of current that panel can provide when irradiation changes. This change in available current is modelled by controlling external current source in parallel to the PV-panel model. Layout of this arrangement is represented in Figure 11.

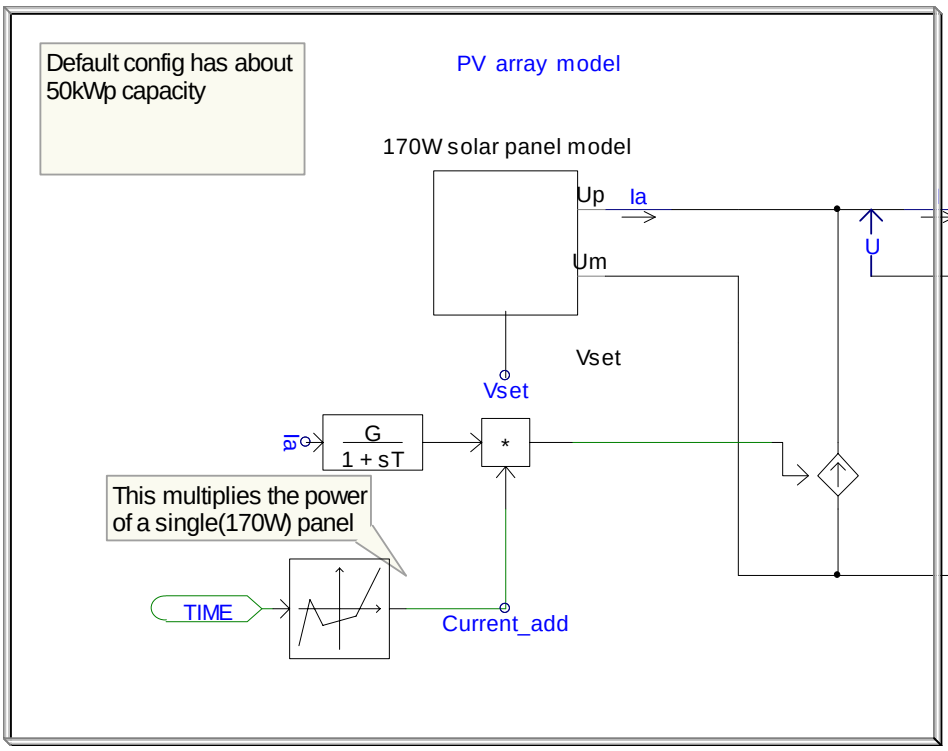

Figure 11. Layout of PV array model.

PV panel model is responsible of voltage current characteristics and external current source is used to multiply and change available current when irradiation changes are wanted to be modelled. As default the maximum power value is set to 50kW but there should not be any problems with the model to higher or lower by adjusting Current_add parameter.

3.1.4 Idea behind parallel connection of panels

Maximum power point tracking (MPPT) means tracking of optimum operation point for the solar panel system in UI-curves. In practice this means controlling DC/DC converter of the solar system so that MPP is achieved and solar power generation yield maximised. Figure 12 displays voltage and current characteristics of the PW1650 module under different irradiation conditions [3].

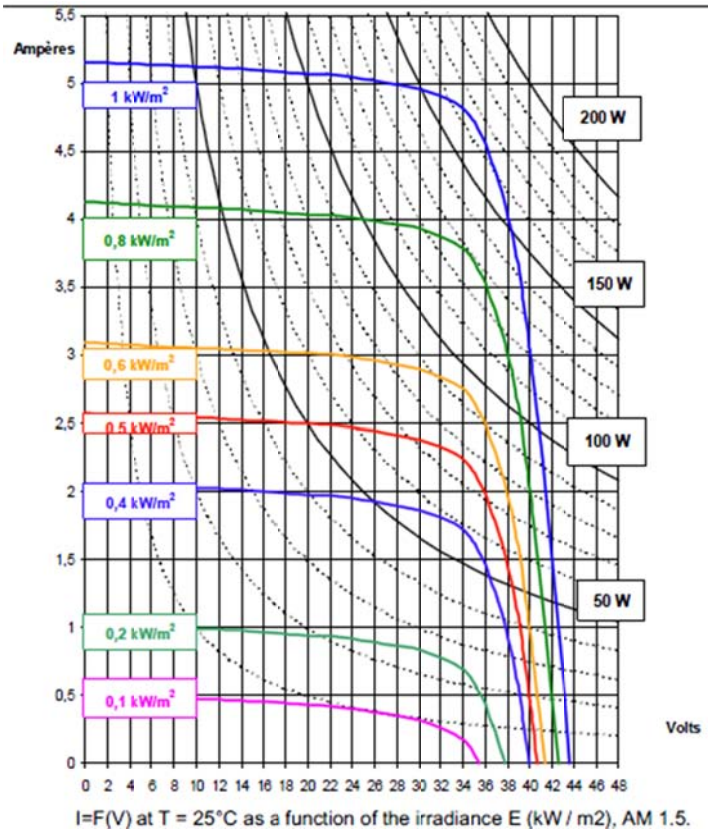

Figure 12. UI characteristics of PW1650 [3].

The figure illustrates that maximum power point is found around the bend of the UI-curve but actual values of voltage and current differ respect to irradiation, which is of course understandable as available power changes. Notable fact however is that current of the panel at maximum power points ranges from 0.4A to 5.5A which means highest value of current is 1275% larger than the lowest. Voltage range at MPPs is between 28V to 35V which means the highest voltage is only 25% higher than the lowest.

In parallel connection of solar panels, UI-curve of the system remains close to the shape of the individual panels like the one represented in Figure 12. This shape also remains fairly well under different irradiation situations and shading. On series connection of panels, the system UI-curve shape changes much more respect to shading. Comparisons have been made in many articles between parallel and series connection of panels like in [5] and in [6]. The studies show that parallel connection of panel offers the superior performance between these two and especially under heavily shaded conditions.

These two facts led to decisions to use parallel connection of panels and voltage control in DC/DC converter. Voltage control is safer option compared to adjusting current because right voltage is within narrow range, and even when the voltage is not

exactly on maximum power point, it is always fairly close and wasted energy is smaller if tracking fails.

3.1.5 DC/DC converter model for solar array

DC/DC converter chosen for the solar array is boost type converter but with controllable voltage on both output nodes. In practice this means using two boost converters which give symmetrical but complement output voltages respect to ground. Circuit layout of the converter is represented in Figure 13.

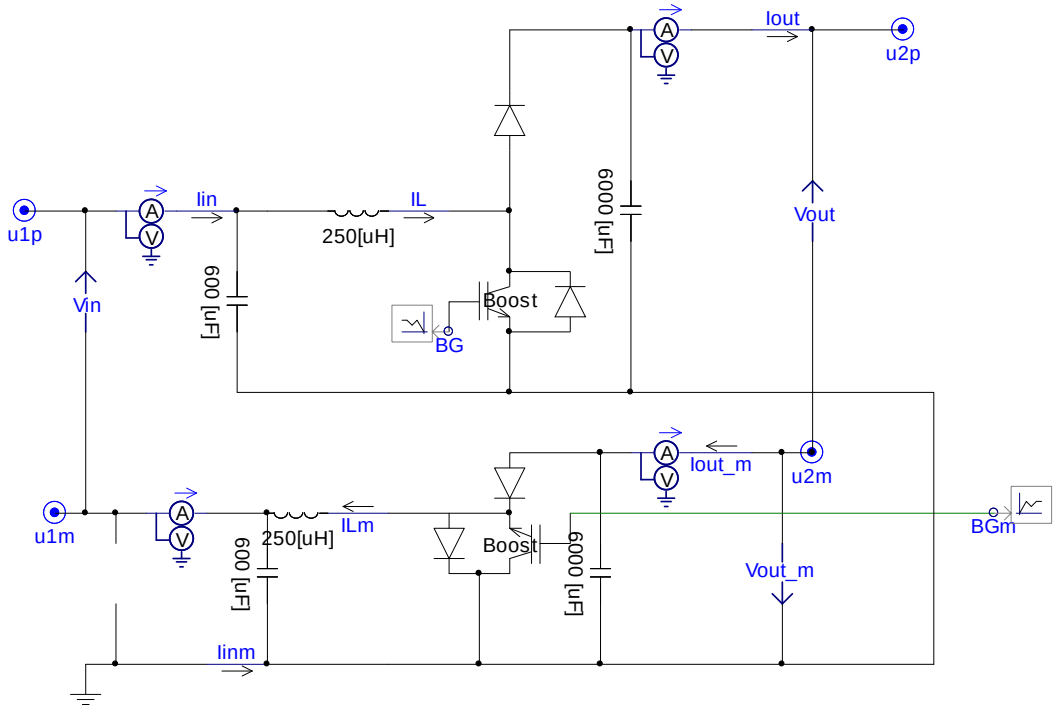

Figure 13. Circuit layout of DC/DC converter for solar array.

Like mentioned in previous chapter, the converter is controlled by controlling input voltage. This maximum power point tracking method is known better as constant voltage control. In this control, the input voltage is measured and current reference is increased or decreased until input voltage meets the predefined value. Actual switching signal is generated on demand by variable frequency comparator. The usual method would be to use duty ratio control with static frequency control. Layout of constant voltage MPPT control is represented in Figure 14.

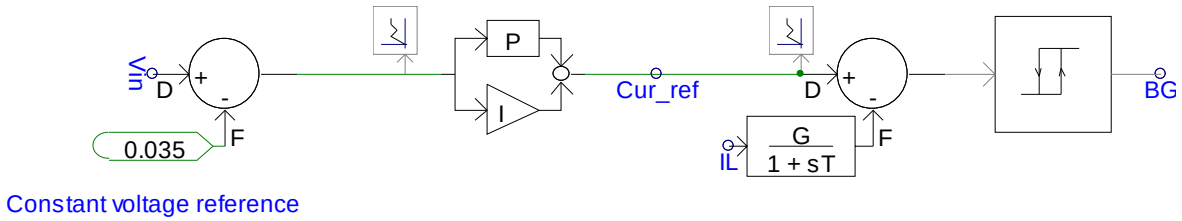

Figure 14. Control of constant voltage MPPT with variable frequency.

Voltage difference to reference voltage is used as input for PI controller, which output is compared to inductor current. Difference of current and reference is given to tolerance band comparator to generated switching signal. Concept of this control method is described in [7] at pages 337–341.

3.2 Boost converter between inverter and DC-side

A boost converter is connected between Grid and DC side. The converter boosts voltage from 50V to 1000V. Converter operates at variable frequency with tolerance band control like the one used in connecting solar array model. Circuit layout is displayed in Figure 15.

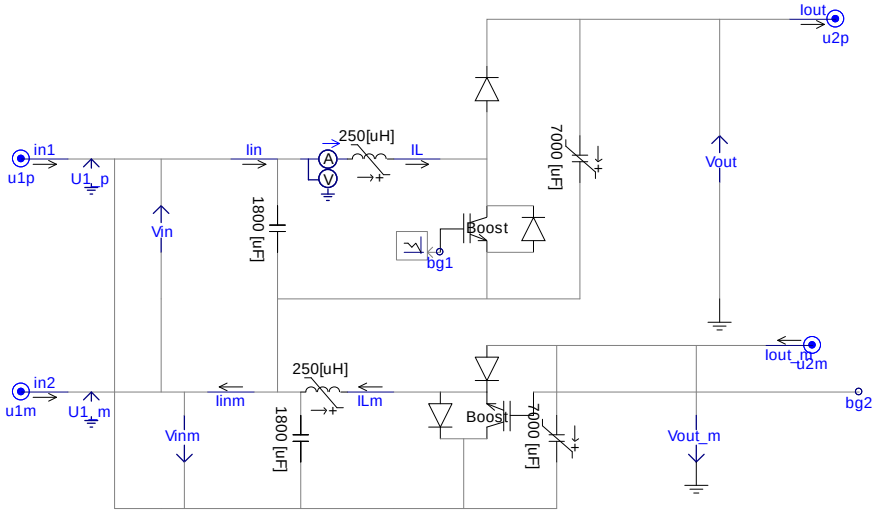

Figure 15. Boost converter between DC-side and inverter.

The difference between this and solar panel converter is that both IGBTs switch between +- DC nodes and not between node and ground. This results to an improved response and lower required boost multiplier because voltage of input side is higher.

3.3 Island inverter and isolation transformer

Inverter model chosen for the model is based on space vector control with slight modification to common practices. Figure 16 displays simulation blocks of inverter and isolation transformer which is connected between inverter and grid.

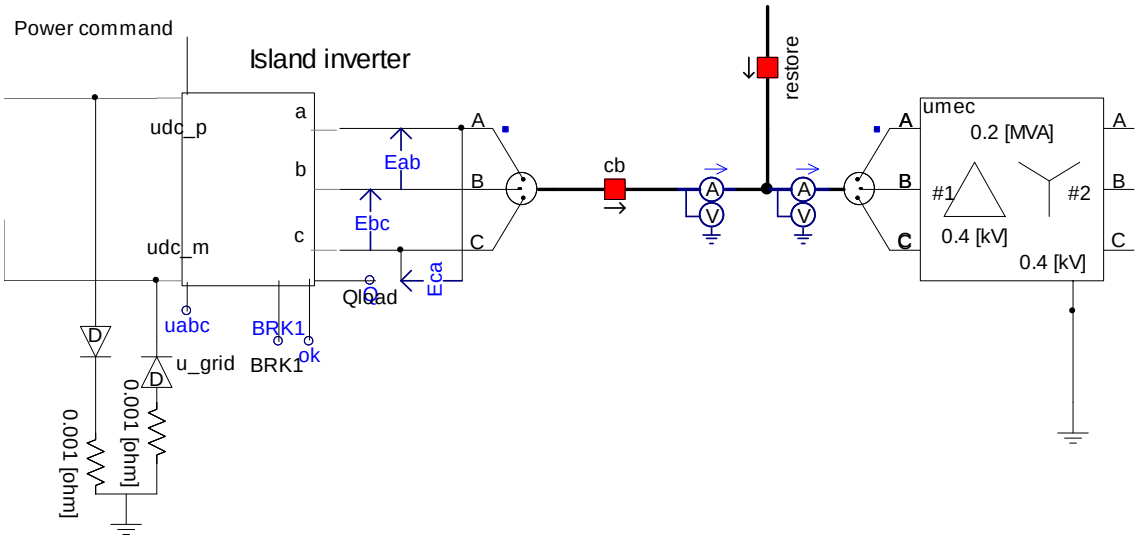

Figure 16. Inverter and isolation transformer.

Delta-wye transformer is used to remove 3rd harmonics from the voltage and generate neutral point for demand side. Passive surge protector is added to DC-line to remove possible voltage spikes in rapid changes of DC/DC converter output. After the transformer there is a 400 W wye connected resistive load to model own use of the energy centre (lighting, etc.). Resistive load model with neutral connector can be found at UWASA model library “VYlib42” at SGEM PSCAD library.

3.3.1 Inverter main circuit

Inverter main circuit is displayed in Figure 17. Design is a 2-level inverter with LCL-type filter. L2 is set to be half of L value. Both L and C are adjustable in the model.

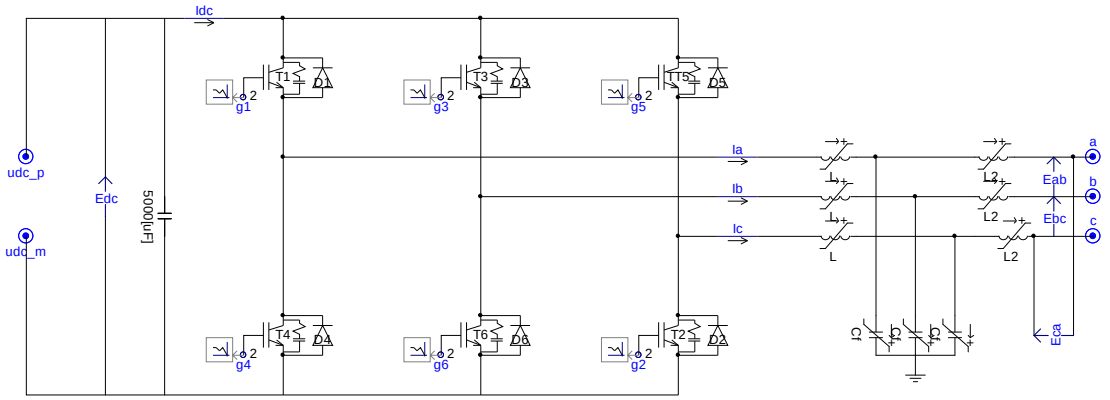

Figure 17. Inverter main circuit.

3.3.2 Inverter control system

Inverter is equipped with two control systems, one for grid parallel operation and one for islanded operation. Control systems are switched when grid side LOM protection relay is tripped on and off. In this model, grid side protection is assumed to work correctly when there is fault in grid.

Inverter control system for islanded operation is displayed in Figure 18. Design principle of the inverter control system was to achieve best possible response to fast load changes. Power quality is kept good by LCL-filter of the inverter, high switching frequency and Delta wye transformer.

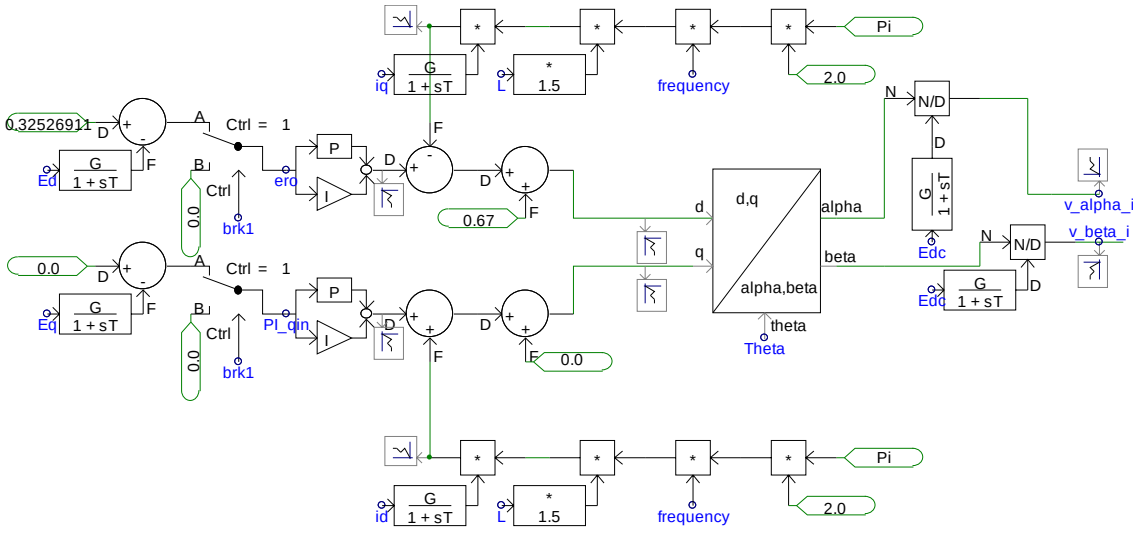

Figure 18. Inverter control system for islanded operation.

Control logic was made to control voltage with two PI-controllers. This control type can also be called single-loop control [8]. DQ component representation is used in control

system. Transformation to DQ system from 3-phase values can be done with following matrix equation 3.

$$\begin{bmatrix} U_D \\ U_Q \\ U_0 \end{bmatrix} = \frac{2}{3} \begin{bmatrix} \cos(\phi) & \cos(\phi - \frac{2\pi}{3}) & \cos(\phi - \frac{4\pi}{3}) \\ -\sin(\phi) & -\sin(\phi - \frac{2\pi}{3}) & -\sin((\phi - \frac{4\pi}{3}) \\ \frac{1}{2} & \frac{1}{2} & \frac{1}{2} \end{bmatrix} \begin{bmatrix} Ua \\ Ub \\ Uc \end{bmatrix}$$

Equation 3. ABC to DQ transformation [9].

To reduce spikes during switch from and to islanded operation, PI controllers are driven to zero when control system is not used. In symmetric 400V AC system, Ed component is same as peak value of phase voltage and Eq component is zero, when angle in transformation matrix is locked to *Ua* angle. These reference values are given to islanded inverter control system.

Control system in grid parallel operation is represented in Figure 19. Control system is based on decoupled active and reactive power control.

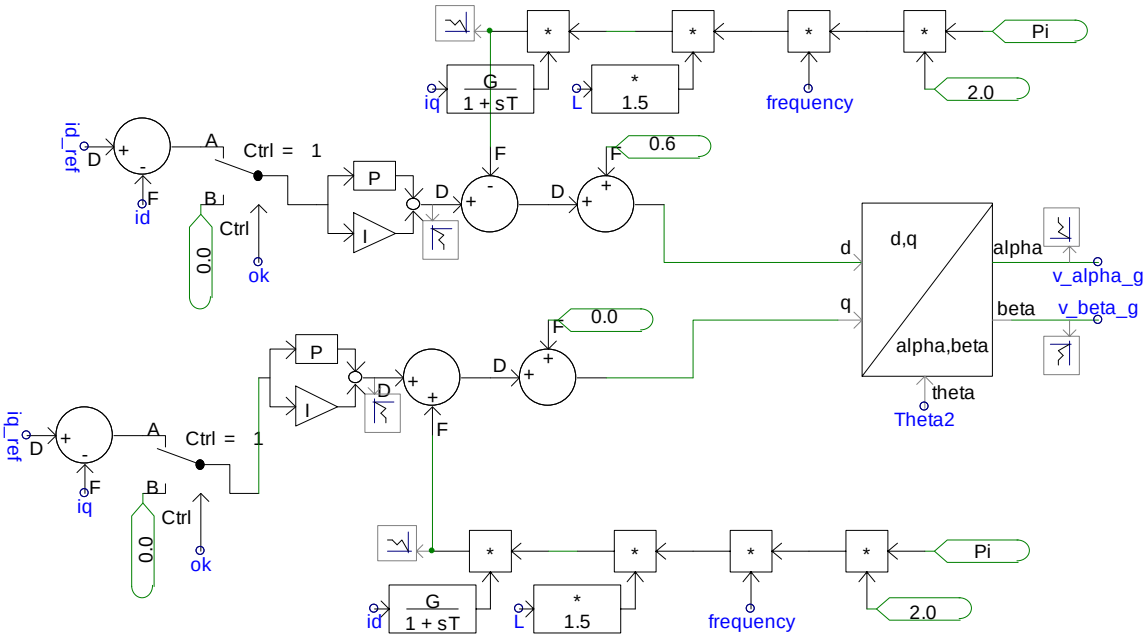

Figure 19. Control system for grid parallel operation.

Control system is based on one represented in [8]. Current references are calculated with following equations from power references.

$$id\_ref = \frac{2 \cdot P}{3 \cdot ud}$$

$$iq\_ref = \frac{2 \cdot Q}{3 \cdot ud}$$

Active power reference is given by DC-unit and reactive power reference is same as measured reactive power consumption of demand side to minimise reactive power flow from outside grid.

3.3.3 Synchronisation system

Synchronisation is required so that there are no spikes and fast phase angle changes during connection of system to outside grid and back to islanded mode. Phase angle reference of islanded mode is adjusted to follow outside grid phase angle when there are no faults in outside grid. This way switch to islanded mode can be done without sudden phase angle change in loads. Also phase angle of islanded mode is adjusted to match outside grid before reconnecting system back to rest of the distribution system. Figure 20 represents synchronisation system in the model.

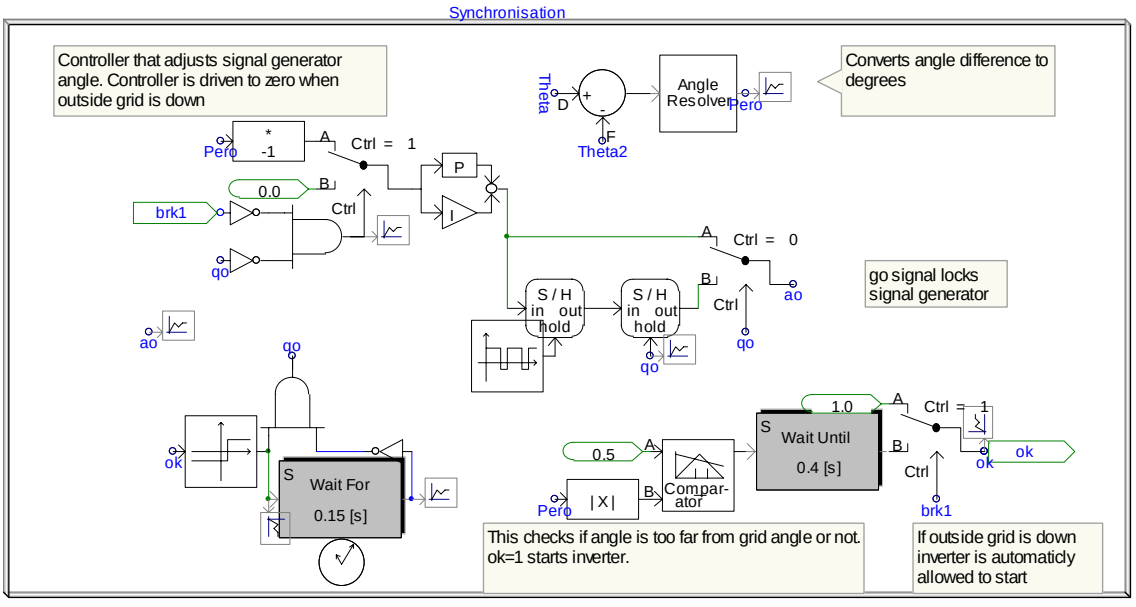

Figure 20. Synchronisation system in the model.

Related to synchronisation, there is a switch called “restore” between grid and inverter. This switch will remain open unless phase angle difference is small enough between grid and inverter.

3.3.4 Other details

Switching frequency of the space vector modulator is 15 kHz. Note that filtering must be increased if switching frequency is wanted to be adjusted lower. Inverter operating mode can be switched between 60 Hz and 50 Hz but filtering, grid model and transformer settings are adjusted to 50 Hz operation by default.

3.4 Demand side

Demand side is consists of 4-wire line and adjustable resistive load component at the end of the line. Figure 21 displays demand side grid model.

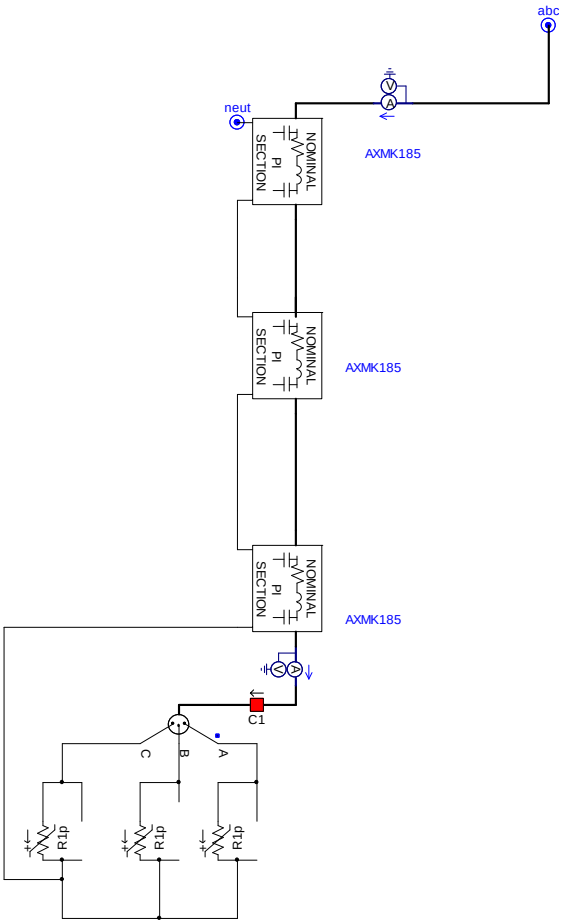

Figure 21. Demand side grid model.

Lines are AXMK185 ground cable. Load resistance is adjusted according to power reference and calculated by following computation.

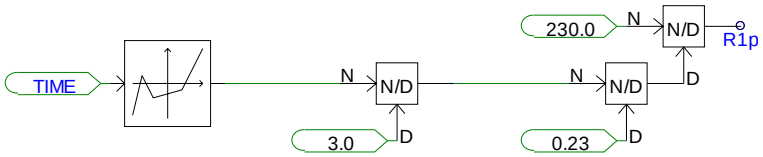

Figure 22. Load resistance calculation from power reference.

4. Simulation results

Following simulation results describe a case where solar power production alters and load is also changing at same time in demand side. Fault occurs at grid at 4.5s and inverter then switches to islanded mode. Outside grid heals at 7.5s and then inverter switches back to power control mode and synchronises to grid voltages.

4.1 DC side results

Figure 23 represents output power of the solar panel array and how well it can follow available irradiation power.

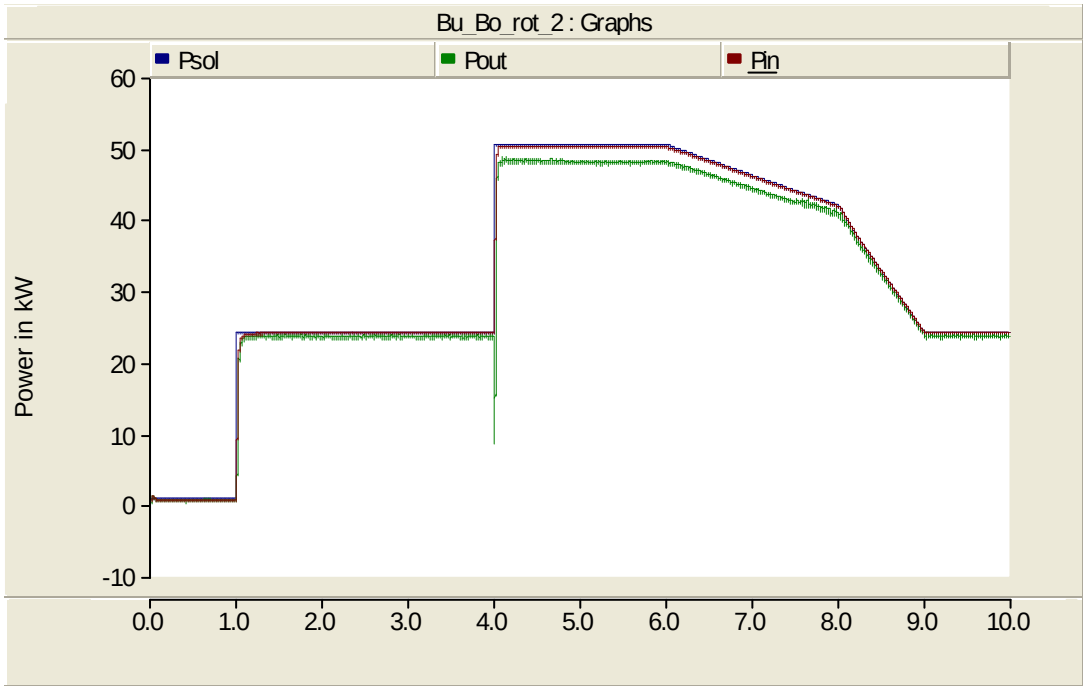

Figure 23. Solar array power (red), available power to be converted (blue), and power output of the DC/DC converter (green).

State of charge (SOC) of the battery is displayed in Figure 24.

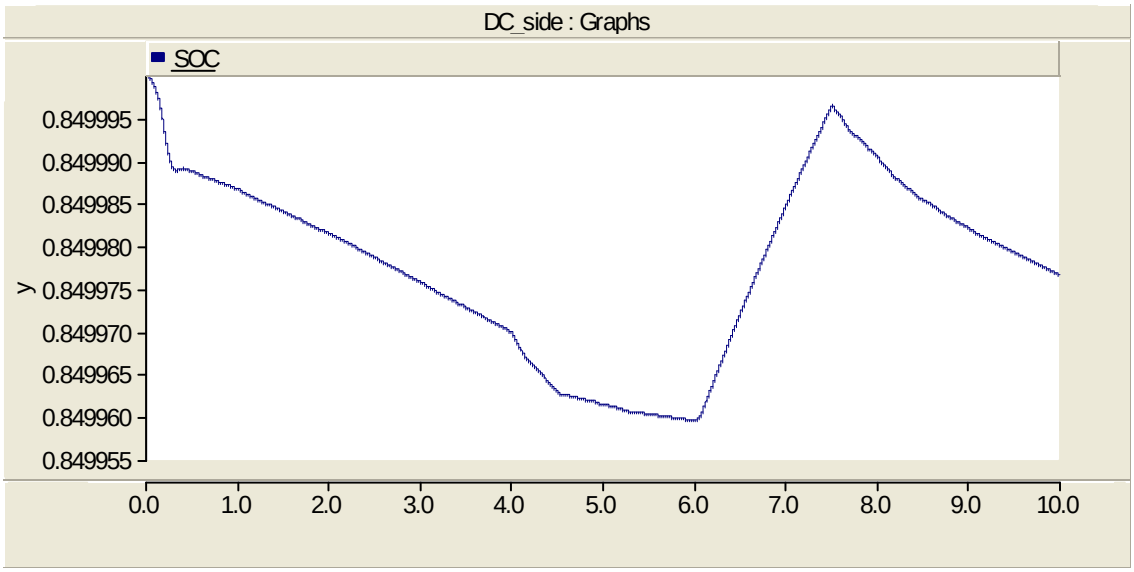

Figure 24. State of charge of the battery unit.

Voltage of the DC side represented in Figure 25 is fluctuating when solar power output changes and inverter power output changes. DC voltage supplied to inverter is represented in Figure 26.

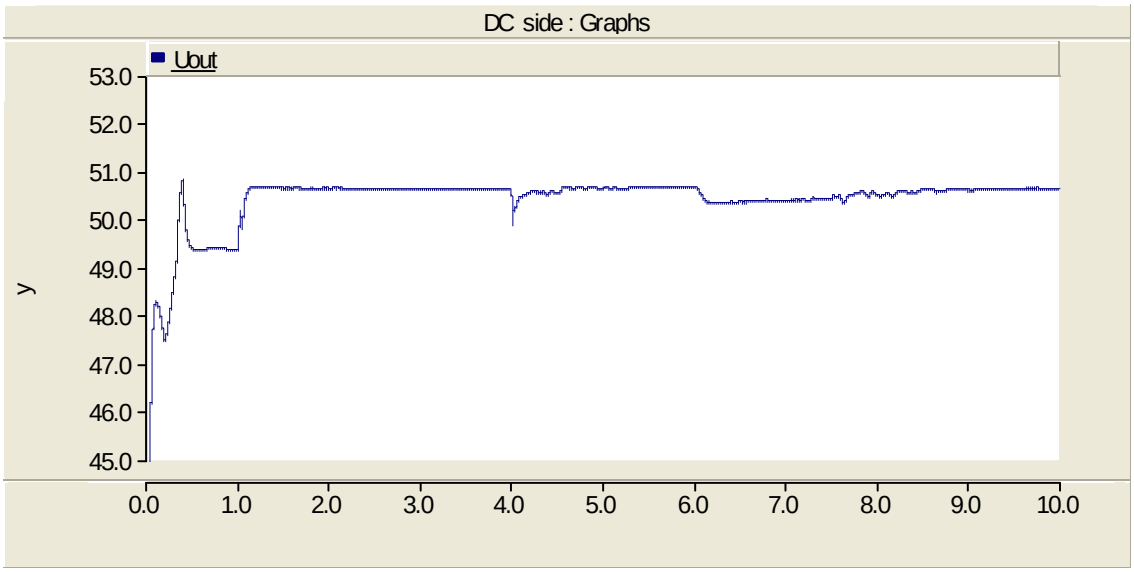

Figure 25. Voltage at “50V” DC lines.

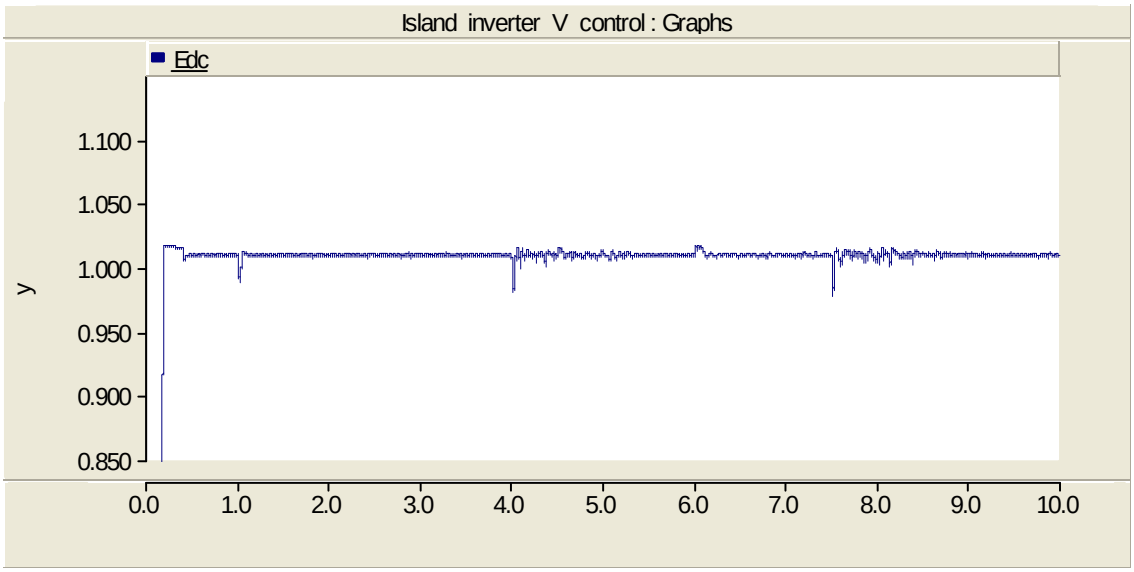

Figure 26. Voltage after boost converter between DC-side and inverter in kV.

4.2 AC side results

A sample of the output voltage is represented in Figure 27.

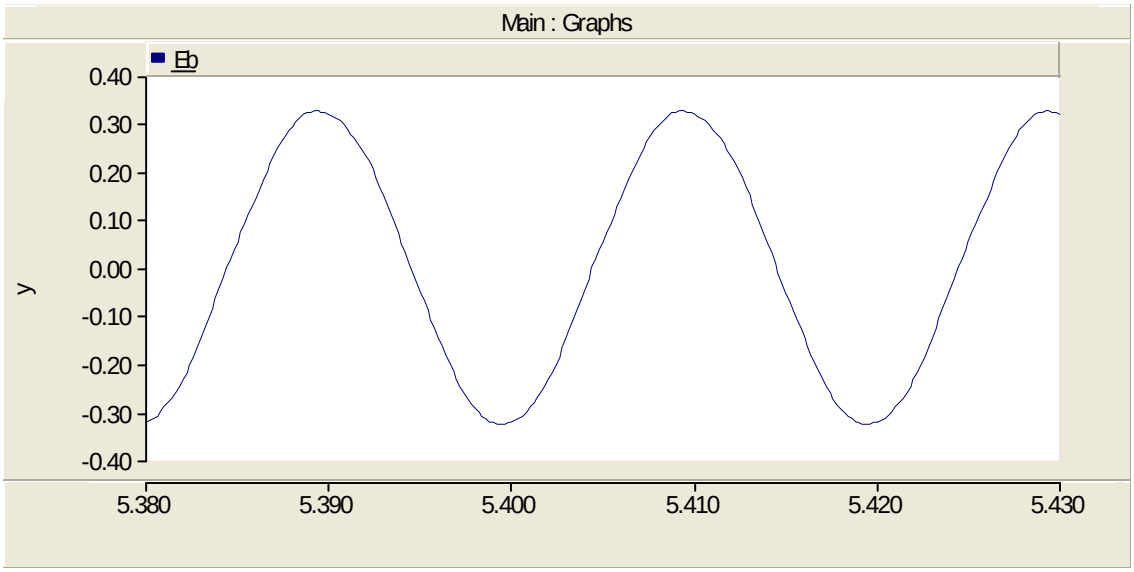

Figure 27. Sample of the AC voltage.

Figure 28 displays the voltage during fault occurs in the grid and inverter switches to islanded mode.

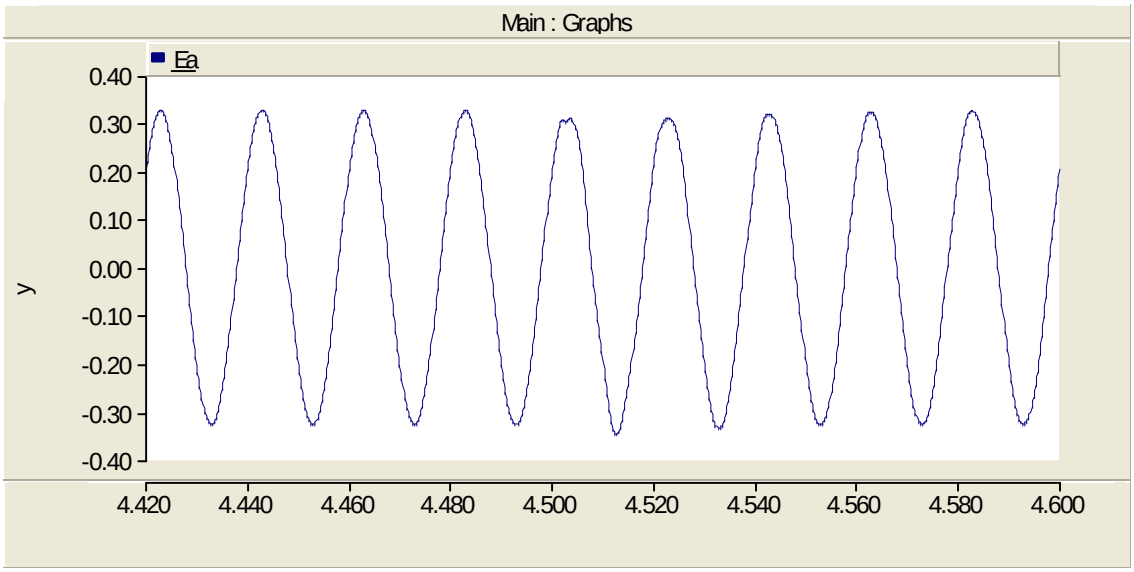

Figure 28. Voltage during grid fault and transition to islanded mode.

RMS base frequency line voltage in kV is represented in Figure 29. Quick flicker at 4.5s is result of fault in grid and inverter switching to islanded mode.

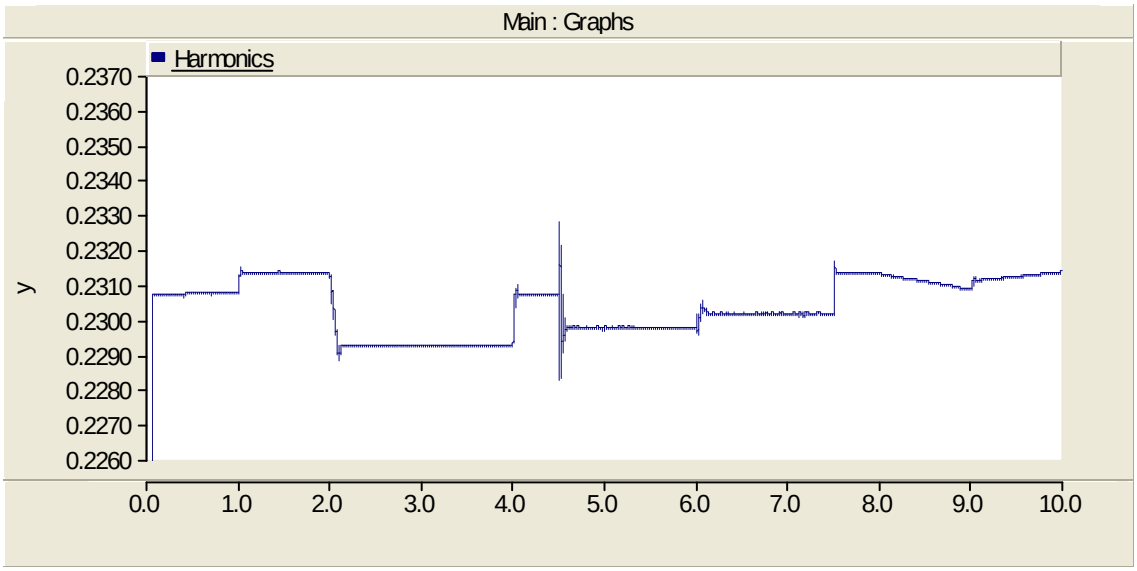

Figure 29. RMS value of 50 Hz component of load voltage.

Power consumption of loads is represented in Figure 30. Blue is active power in kW and green is reactive power in kVAr.

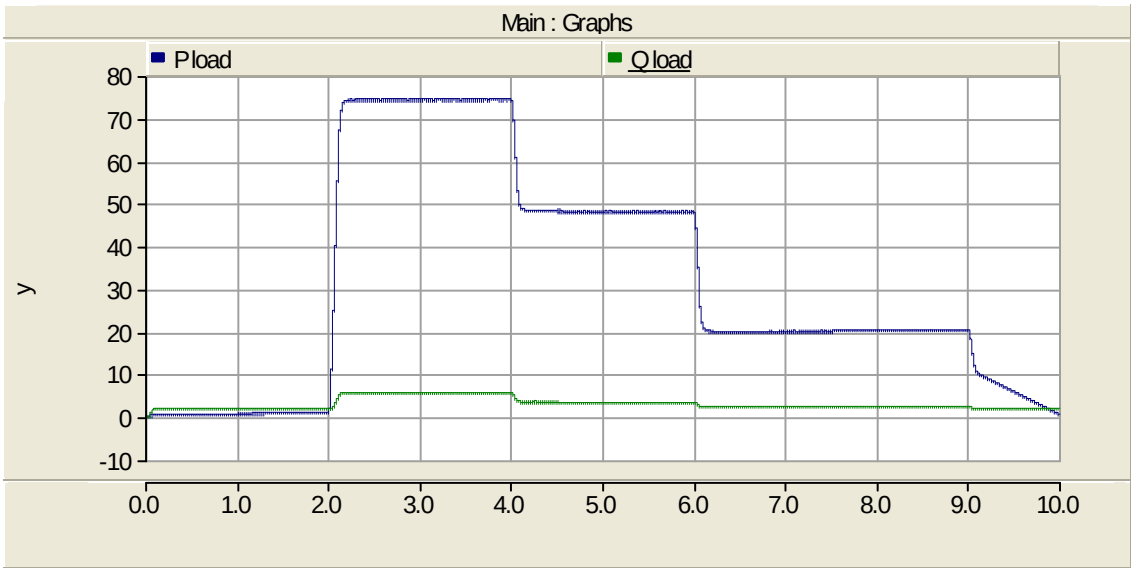

Figure 30. Power consumption of loads. Active power (P) in blue [kW], reactive power(Q) in green[kVar].

Inverter power output is represented in Figure 31.

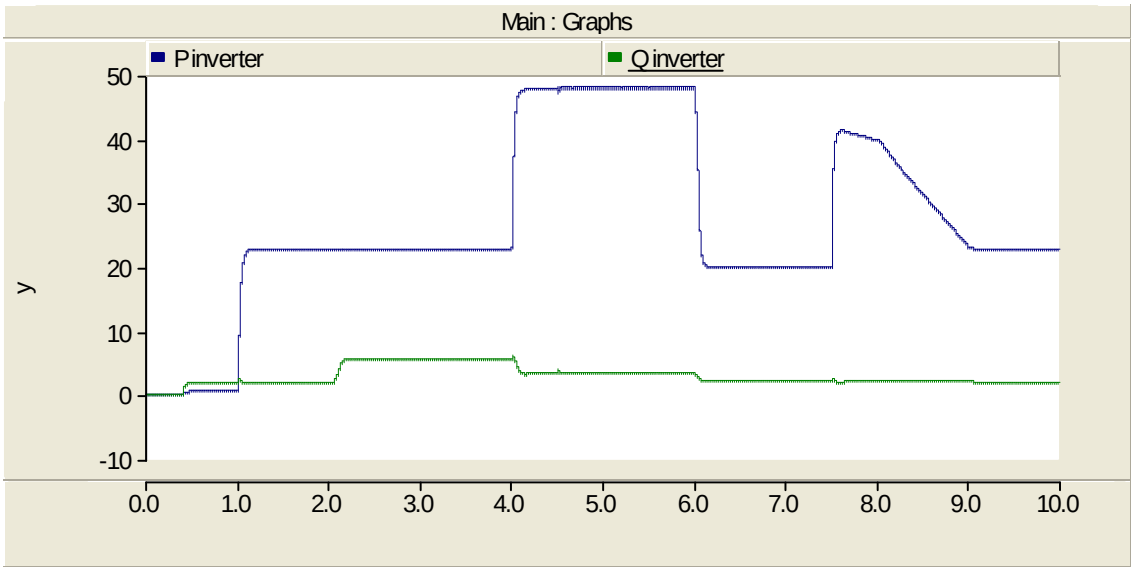

Figure 31. Inverter power output. Active power (P) in blue [kW], reactive power (Q) in green [kVar].

Total harmonic distortion (THD) is displayed in Figure 32. THD is calculated from 63 harmonics and compared to base frequency component. Figure shows high spike when fault occurs in the grid. Grid connection is restored at 7.5s which shows as small spike in the figure.

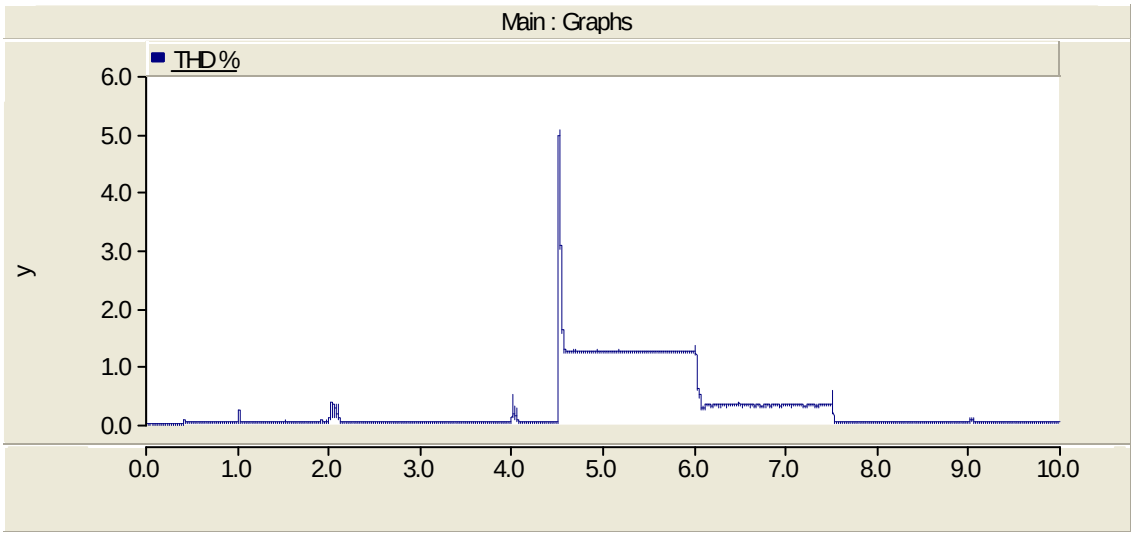

Figure 32. Total harmonic distortion calculated up to 63rd harmonic and compared to base frequency signal.

5. Summary

A simulation model of Energy centre microgrid made with PSCAD simulation software version 4.2.1 has been built in SGEM Smart Grids and Energy Markets (SGEM) work package 6.6. Microgrid is an autonomous electric power system which can operate separate from common distribution system. The idea of energy centre microgrid concept was considered in Master of Science thesis “Community Microgrid – A Building block of Finnish Smart Grid”. The name of energy centre microgrid comes from a fact that production and storage units are concentrated into a single location, an energy centre. This centre feeds the loads which can be households or industrial loads. Power direction flow on the demand side remains same compared to the current distribution system and allows to the use of standard fuse protection in the system.

The model consists of photovoltaic solar array, battery unit, variable frequency boost converter, inverter, isolation transformer and demand side (load) model. The model is capable to automatically switch to islanded mode when there is a fault is outside grid and back to parallel operation mode when fault is removed. The modelled system responses well to load changes and total harmonic distortion related to 50Hz base frequency is kept under 1.5% while operating and feeding passive load.

Improvements to the model can be made by implementing realistic grid side LOM protection relay as now LOM protection is assumed work correctly. Solar array model accuracy could be improved further and maximum power point tracking method could also be updated from constant voltage control to a method with higher accuracy. The model will be used in next phase of SGEM project to analyse possible phenomena caused by large single phase loads and possibilities to control them smartly in microgrid environment.

References

[1] Pasonen, R. 2010. Community Microgrid – A Building Block of Finnish Smart Grid. Master of Science thesis. Tampere University of Technology, Finland.

[2] Gergaud, O., Rogib, G., Multon, B., Ben Ahmed, H. 2003. Energy modelling of a lead-acid battery within hybrid wind/photovoltaic systems. ENS Cachan, Bruz, France.

[3] Data for photowatt 1650 solar panel. Available at: http://www.proidea.hu/bps-business-power-systems-107698/photowatt-napelemek-252476/PW%201650.pdf (4.10.2011).

[4] Cambell, R., C. 2007. A Circuit-based Photovoltaic Array Model for power system studies. Department of Electrical Engineering. University of Washington, Seattle, WA, USA.

[5] Oldenkamp, H., de Jong, I. van der Borg, N. 2004. PV-wirefree versus conventional PV-systems: Detailed analysis of difference in energy yield between series and parallel connected PV modules. OKE-Services(1) and Energy research Centre of the Netherlands(2), 19th European Photovoltaic Solar Energy Conference and Exhibition, Paris, France, 7–11 June, 2004.

[6] Ramaprabha, R., Gandhi Salai, R. 2009. Effect of Shading on Series and Parallel Connected Solar PV Modules. Canadian Center of Science and Education. Modern Applied Science, 3(10).

[7] Mohan, N., Undeland, T., Robbins, W. 2009. Power electronics – Converters, Applications, and Design. Wiley, India.

[8] Green,T., Prodanovic, M. 2007. Control of inverter-based micro-grids. Electric Power Systems Research, 77(9). Distributed Generation.

[9] Luomi, J. 1982. Sähkökoneiden muutosilmiöt 816 B. Otakustantamo, Finland. (In Finnish.)

VTT Working Papers

168 Pekka Leviäkangas, Anu Tuominen, Riitta Molarius & Heta Kajo (Eds.). Extreme weather impacts on transport systems. 2011. 119 p. + app. 14 p.

169 Luigi Macchi, Elina Pietikäinen, Teemu Reiman, Jouko Heikkilä & Kaarin Ruuhilehto. Patient safety management. Available models and systems. 2011. 44 p. + app. 3 p.

170 Raine Hautala, Pekka Leviäkangas, Risto Öörni & Virpi Britschgi. Perusopetuksen tietotekniikkapalveluiden arviointi. Kauniaisten suomenkielinen koulutoimi. 2011. 67 s. + liitt. 16.

171 Anne Arvola, Aimo Tiilikainen, Maiju Aikala, Mikko Jauho, Katja Järvelä & Oskari Salmi. Tulevaisuuden elintarvikepakkaus. Kuluttajalähtöinen kehitys- ja tutkimushanke. 152 s. + liitt. 27 s.

172 Sauli Kivikunnas & Juhani Heilala. Tuotantosimuloinnin tietointegraatio. Standardikatsaus. 2011. 29 s.

173 Eetu Pilli-Sihvola, Mikko Tarkiainen, Armi Vilkman & Raine Hautala. Paikkasidonnaiset liikenteen palvelut. Teknologia ja arkkitehtuurit. 2011. 92 s.

174 Eetu Pilli-Sihvola, Heidi Auvinen, Mikko Tarkiainen & Raine Hautala. Paikkasidonnaiset liikenteen palvelut. Palveluiden nykytila. 2011. 59 s.

175 Armi Vilkman, Raine Hautala & Eetu Pilli-Sihvola. Paikkasidonnaisten liikenteen palveluiden liiketoimintamallit. Edellytykset, vaihtoehdot, haasteet ja mahdollisuudet. 2011. 49 s. + liitt. 2 s.

176 Henna Punkkinen, Nea Teerioja, Elina Merta, Katja Moliis, Ulla-Maija Mroueh & Markku Ollikainen. Pyrolyysin potentiaali jätemuovin käsittelymenetelmänä. Ympäristökuormitukset ja kustannusvaikutukset. 79 s. + liitt. 15 s.

177 Kim Björkman, Janne Valkonen & Jukka Ranta. Model-based analysis of an automated changeover switching unit for a busbar. MODSAFE 2009 work report. 2011. 23 p.

178 Anders Stenberg & Hannele Holttinen. Tuulivoiman tuotantotilastot. Vuosiraportti 2010. 2011. 46 s. + liitt. 5 s.

179 Alpo Ranta-Maunus, Julia K. Denzler & Peter Stapel. Strength of European Timber. Part 2: Properties of spruce and pine tested in Gradewood project. 2011. 67 p. + app. 46 p.

180 Pasi Valkokari, Toni Ahonen, Heljä Franssila, Antti Itäsalo, Jere Jännes, Tero Välisalo, Asko Ellman. Käyttövarmuussuunnittelun kehittämistarpeet. Käyttövarmuuden hallinnta suunnitelussa – hankkeen työraportti 1. 2011. 53 s. + liitt. 21 s.

181 Hannu Viitanen, Tommi Toratti, Lasse Makkonen, Ruut Pehkuri, Tuomo Ojanen, Sven Thelandersson, Tord Isaksson & Ewa Früwald. Climate data. Exposure conditions in Europe. 2011. 45 p.

182 Riku Pasonen. Energy centre microgrid model. 2011. 34 p.

ISBN 978-951-38-7524-4 (URL: http://www.vtt.fi/publications/index.jsp)
ISSN 1459-7683 (URL: http://www.vtt.fi/publications/index.jsp)